Aggregate Modeling of System-Level Thermal Demand Flexibility

Catherine Wang, Constance Crozier
School of Industrial & Systems Engineering
Georgia Institute of Technology
Atlanta, GA, USA
catherine.wang@gatech.edu

Priyadarshan Priyadarshan, Kevin Kircher
Department of Mechanical Engineering
Purdue University
West Lafayette, IN, USA
priyada@purdue.edu

***Abstract*—Electrification of residential heating plays an increasingly important role in demand-side management, as heating loads can provide flexibility by shifting or modulating consumption during stressed system periods. However, existing approaches rely on either detailed individual building models or simplified aggregate models that do not consider key thermal dynamics. In this paper, we propose an aggregate thermal model of large-scale residential heating systems. The model captures building thermal flexibility under electricity price signals and incorporates thermal water storage behavior. The proposed model is validated on a French residential heating case study and closely matches Monte Carlo simulations with hourly relative Root Mean Square Errors of 7.81% and 7.64% during cold and mild days and reduced computational time from 5.5 seconds to 0.03 seconds with 1,000 buildings.**

***Index Terms*—Space heating, heat pumps, demand flexibility.**

NOMENCLATURE

Parameters

a	Discrete-time dynamics coefficient
C	Thermal capacitance (kWh/°C)
E	Energy (kWh)
f	Fraction of units
N	Number of units
R	Thermal resistance (°C/kW)
$\mathcal{T}$	Set of time steps in the studied period
T^{in}	Indoor temperature (°C)
T^{out}	Outdoor temperature (°C)
T^{tk}	Tank temperature (°C)
T^{tk}_{amb}	Ambient temperature surrounding the tank (°C)
Δt	Time interval (h)
η	Coefficient of performance
λ	Electricity price ($/kWh)
τ	Time constant (h)
Φ	Exogenous heat gains (kW)

Decision Variables

E^{tk}_t	Tank energy at time t (kWh)
p^{hp}_t	Heat pump electrical power at time t (kW)
p^{res}_t	Resistive heater electrical power at time t (kW)
q^{AA}_t	Air-to-air thermal power at time t (kW)
$q^{AW,c}_t$	Tank charging thermal power at time t (kW)
$q^{AW,d}_t$	Tank discharging thermal power at time t (kW)
q^{total}_t	Total building thermal power at time t (kW)
T^{in}_t	Indoor temperature at time t (°C)

Notation

AA	Air-to-air
agg	Aggregate level
AW	Air-to-water
$bldg$	Building
c	Charging
d	Discharging
hp	Heat pump
res	Resistive heating
tk	Water tank
$total$	Total heating
$cold$	Cold
$final$	Final value
hot	Hot
$init$	Initial value
$\max$	Maximum value
$\min$	Minimum value
t	Discrete time step

I. INTRODUCTION

Electrification and expansion of renewable energy generation are key drivers of power system decarbonization, but they also introduce operational challenges due to the added variability in both supply and demand. Demand-side flexibility has emerged as a critical resource for balancing supply and demand and maintaining reliable systems during stressed periods and extreme weather events [1]. Among demand-side resources, buildings, particularly heating, ventilation, and air-conditioning (HVAC) systems, represent a major source of flexibility, as their electricity consumption can be modulated or shifted over time in response to price signals. Thus, thermal flexibility provides opportunities for peak demand reduction and improved system planning and operation [2].

The flexibility of buildings arises mainly from their thermal inertia and thus ability to store thermal energy within the building structure. As these thermal dynamics are affected by weather conditions, occupant behavior, building characteristics, and HVAC system operation, researchers have developed a range of modeling approaches, including physics-based models and data-driven models [3]–[5]. Since indoor temperatures can vary within acceptable comfort bounds, HVAC systems can temporarily shift electricity consumption over time without significantly affecting occupant comfort. In practice, this flexibility can be achieved through operational strategies such as thermostat setpoint adjustments [6], preheating or pre-cooling [7], and load shifting in response to incentives [8].

At the system level, flexibility arises from a large population of buildings rather than individual units, motivating studies that approximate aggregate thermal flexibility [9]. Prior work has shown that aggregating residential heating systems can enhance system flexibility, enabling applications such as coordinated control strategies [10], provision of grid services such as frequency regulation [11], and peak demand reduction through the large-scale deployment of smart thermostats [12]. However, most existing methods either rely on detailed models of individual buildings, or abstract away the underlying thermal dynamics of building populations [13]. Building-level models capture heterogeneous thermal behavior but are computationally expensive for large-scale studies, whereas aggregate models often simplify the thermal dynamics (e.g., ignoring device variation) and therefore limit their ability to realistically represent flexibility during stressed periods.

In this paper, we propose an aggregate thermal modeling framework to represent the collective flexibility of residential heating systems in large-scale power system analysis. Our contributions can be summarized as:

- We develop an aggregate thermal model that captures the flexibility of large populations of HVAC systems.
- We incorporate both air-to-air and air-to-water heat pump systems, including thermal water storage, to represent additional sources of flexibility.
- We validate the proposed framework against a Monte Carlo (MC) benchmark using a French case study and demonstrate its ability to accurately reproduce system-level thermal behavior with lower computational cost.

II. Building Thermal Controls

Here we first present the thermal dynamics of a single building and then extend the formulation to an aggregate model. We consider two common types of heat pumps: air-to-air and air-to-water, each supplemented with an independent resistive heating source. The indoor temperature dynamics of buildings are modeled using a first-order resistance-capacitance (RC) formulation with a discrete time interval Δt [1]:

$$T_{t+1}^{in} = a^{bldg} T_t^{in} + (1 - a^{bldg}) R^{bldg} \left(q_t^{total} + \Phi_t + \frac{T_t^{out}}{R^{bldg}}\right), \quad (1)$$

where $\tau^{bldg} = R^{bldg} C^{bldg}$ and $a^{bldg} = e^{-\frac{\Delta t}{\tau^{bldg}}}$. T_t^{in} denotes the indoor temperature per time step t, and T_t^{out} denotes the outdoor air temperature which is assumed to be known over the studied period $\mathcal{T}$. R^{bldg} and C^{bldg} denote the building thermal resistance and capacitance, q_t^{total} denotes the supplied thermal power by all controlled heating equipment, and Φ_t captures exogenous heat gains. In this study, we only focus on heating operations and therefore neglect Φ_t in optimization models and exclude cooling dynamics.

The indoor temperature is bounded by predetermined minimum and maximum allowable temperatures $T_{\min}^{in}$ and $T_{\max}^{in}$, and the terminal indoor temperature is constrained to match the initial temperature in order to prevent artificial energy depletion at the last time step:

$$T_{\min}^{in} \leq T_t^{in} \leq T_{\max}^{in}, \quad T_{init}^{in} = T_{final}^{in}. \quad (2)$$

The general building temperature dynamics above apply to all heating technologies. The following subsections specify technology-dependent state equations and associated constraints. Each technology can be formulated as an individual optimization model, which later allows the models to be combined within the aggregate framework.

A. Air-to-air heat pumps

For an air-to-air system with a resistive heater, the total thermal power q_t^{total} in (1) is delivered directly to the indoor space and is defined as:

$$q_t^{total} = q_t^{AA} + \eta^{res} p_t^{res} = \eta^{hp}(T_t^{out}) p_t^{hp} + \eta^{res} p_t^{res}, \quad (3)$$

where q_t^{AA} denotes the thermal output from the air-to-air equipment and depends on the coefficient of performance (COP) as a linear function of outdoor temperature $\eta^{hp}(T_t^{out})$ and its electrical power p_t^{hp}. The resistive heater operates with constant efficiency η^{res}, and p_t^{res} denotes its electrical power. Both devices are constrained by their rated electrical limits:

$$0 \leq p_t^{hp} \leq p_{\max}^{AA}, \quad 0 \leq p_t^{res} \leq p_{\max}^{res}. \quad (4)$$

B. Air-to-water heat pumps

For an air-to-water device with a resistive heater, the total thermal power q_t^{total} in (1) is assumed to be delivered indirectly through a water storage tank that transfers heat from the air-source heat pump to the indoor space and directly through the resistive heater and is defined as:

$$q_t^{total} = q_t^{AW,d} + \eta^{res} p_t^{res}, \quad (5)$$

where $q_t^{AW,d}$ is the discharging thermal power supplied from the water tank to the building.

The tank is modeled as lumped sensible thermal storage with uniform temperature [14]. The discrete-time tank energy dynamics with $\tau^{tk} = R^{tk} C^{tk}$ and $a^{tk} = e^{-\frac{\Delta t}{\tau^{tk}}}$ are given by

$$E_{t+1}^{tk} = a^{tk} E_t^{tk} + (1 - a^{tk}) \tau^{tk} \left(q_t^{AW,c} + \frac{T_{amb}^{tk} - T_{cold}^{tk}}{R^{tk}} - q_t^{AW,d}\right). \quad (6)$$

E_t^{tk} denotes the tank energy at time t, and R^{tk} and C^{tk} are the tank wall thermal resistance and storage medium thermal capacitance. T_{amb}^{tk} is the constant ambient temperature surrounding the tank, and T_{cold}^{tk} is the tank minimum allowable temperature and used as the energy reference, such that the minimum stored energy is defined as zero. $q_t^{AW,c}$ is the charging thermal power from the air-source heat pump to the tank, and we assume discharging is almost fully efficient due to negligible pump and fan energy contributions.

Tank energy is bounded by the predefined allowable range:

$$0 \leq E_t^{tk} \leq C^{tk}(T_{hot}^{tk} - T_{cold}^{tk}). \quad (7)$$

Similar to (2), the terminal energy E_{final}^{tk} is constrained as

$$E_{init}^{tk} = E_{final}^{tk}. \quad (8)$$

Both devices' charging and discharging thermal and electrical power are constrained:

$$0 \leq q_t^{AW,c} \leq \eta^{hp}(T_t^{out})p_t^{hp}, \quad 0 \leq q_t^{AW,d} \leq q_{\max}^{AW,d}, \tag{9}$$

$$0 \leq p_t^{hp} \leq p_{\max}^{AW}, \quad 0 \leq p_t^{res} \leq p_{\max}^{res}. \tag{10}$$

C. Objective function

For each technology, the optimization model minimizes total electricity cost over the period $\mathcal{T}$:

$$\min \sum_{t \in \mathcal{T}} \lambda_t (p_t^{hp} + p_t^{res}) \Delta t, \tag{11}$$

subject to constraints described above, where the electricity prices λ_t are assumed to be known.

III. Aggregate Thermal Model Framework

In this section, we develop an aggregate model derived from the individual building formulation. Such models are essential for large-scale power system analysis, where modeling thousands or millions of individual buildings leads to heavy computational burden. The goal is to construct an equivalent building representation that approximates the collective response of a population of buildings. This is achieved by using a single indoor temperature state and allowing a mixture of air-to-air and air-to-water systems defined by a predefined ratio, with the same objective function defined in Section II-C.

A. Aggregate thermal model formulation

Let N_{hp} denote the total number of heat pump devices. f^{AA}, f^{AW}, and f^{res} represent the proportions of air-to-air, air-to-water, and resistive heating sources, with $f^{AA} + f^{AW} = 1$ and $0 \leq f^{res} \leq 1$ under the assumption that each building has exactly one primary heat pump and optionally a resistive heater. The corresponding numbers of devices are

$$N^{AA} = f^{AA} N_{hp}, \quad N^{AW} = f^{AW} N_{hp}, \quad N^{res} = f^{res} N_{hp}.$$

Then the aggregate heating power supplied to the building population from both air-to-air and air-to-water systems is

$$q_t^{total} = q_t^{AA} + q_t^{AW,d} + \eta^{res} p_t^{res}. \tag{12}$$

Assuming thermally independent buildings respond to a common price signal and outdoor temperature, the equivalent aggregate building thermal parameters are scaled with N_{hp}:

$$C^{bldg,agg} = C^{bldg} N_{hp}, \quad R^{bldg,agg} = \frac{R^{bldg}}{N_{hp}}.$$

Substituting these scaled parameters into (1) gives the aggregate indoor temperature dynamics, and (2) is kept unchanged. Similarly, the aggregate tank thermal parameters are scaled with N^{AW}:

$$C^{tk,agg} = C^{tk} N^{AW}, \quad R^{tk,agg} = \frac{R^{tk}}{N^{AW}},$$

and the tank energy dynamics in (6)–(8) follow directly with the substituted parameters. Thermal and electrical power limits are grouped and scaled accordingly with shared COP across heat pumps:

$$0 \leq q_t^{AA} + q_t^{AW,c} \leq \eta^{hp}(T_t^{out})p_t^{hp}, \tag{13}$$

$$0 \leq q_t^{AA} \leq q_{\max}^{AA} N^{AA}, \quad 0 \leq q_t^{AW,d} \leq q_{\max}^{AW,d} N^{AW}, \tag{14}$$

$$0 \leq p_t^{hp} \leq p_{\max}^{AA} N^{AA} + p_{\max}^{AW} N^{AW}, \; 0 \leq p_t^{res} \leq p_{\max}^{res} N^{res}. \tag{15}$$

B. Estimating aggregate building thermal resistance

As presented in Section III-A, several aggregate parameters, such as building thermal capacitance and tank characteristics, can be scaled based on their per-building values with the corresponding total number. In contrast, building-level thermal resistance is dependent on multiple heterogeneous factors, such as weather and local building constructions. Thus, an empirical estimation method is proposed to infer a representative thermal resistance for a given region to mirror its system-level heating behavior.

We mainly focus on periods dominated by heating within the studied area, during which space heating operates continuously and indoor temperature is tightly adjusted by thermostats. Hence, the aggregate electricity demand can reflect building thermal losses. For the purpose of estimating the aggregate building thermal resistance, because indoor temperature variations over a single time step are trivial, we assume $T_{t+1}^{in} \approx T_t^{in}$ with a predefined fixed indoor temperature T^{in}. Moreover, the solar and internal gains are small relative to heating demand during these periods. Under these assumptions, (1) at time t can be reduced to

$$0 = \frac{T_t^{out} - T^{in}}{R^{bldg,agg}} + q_t^{total}. \tag{16}$$

The corresponding electrical power is

$$p_t^{total} = \frac{1}{R^{bldg,agg} \cdot \bar{\eta}} \cdot (T^{in} - T_t^{out}), \tag{17}$$

where $\bar{\eta}$ is the average COP across space-heating technologies. This expression suggests a linear relationship between heating electricity load and the difference between indoor and outdoor temperature. The slope of this fitted line is then defined as

$$slope = \frac{\partial p^{total}}{\partial (T^{in} - T^{out})} = \frac{1}{R^{bldg,agg} \cdot \bar{\eta}}, \tag{18}$$

and is used to compute the aggregate thermal resistance $R^{bldg,agg}$. To relate this quantity to individual buildings, we consider a region contains N electrically heated buildings with similar thermal properties and define a representative per-building thermal resistance R^{bldg} such that

$$\frac{1}{R^{bldg,agg}} \approx \frac{N}{R^{bldg}}. \tag{19}$$

The R^{bldg} can be interpreted as an equivalent per-building resistance consistent with the aggregate estimate.

In practice, total electricity demand includes both temperature-sensitive and temperature-insensitive components (e.g., industry and commercial loads); therefore, even during heating-dominated periods, it can still introduce noise into the regression. The COP also varies with outdoor temperature and technologies. As a result, this proposed aggregate resistance demonstrates a representative thermal parameter instead of a physically grounded resistance of any individual building.

C. Model validation

The accuracy of the aggregate model presented above is evaluated using an MC model as a benchmark. This comparison is intended to evaluate whether the model can capture joint building thermal behavior within a reasonable variability range (rather than able to reproduce the true distribution). In the MC model, each building follows the same optimization formulation described in Section II. Heterogeneity is introduced by independently sampling the temperature bounds $T^{in}_{\min}$ and $T^{in}_{\max}$ from normal distributions centered around chosen setpoints. The indoor temperature inputs in the aggregate model are set to the mean setpoints used in the MC sampling process. For consistency, both the MC and aggregate models are subjected to identical outdoor temperatures and electricity price signals.

IV. Case Study

We apply the proposed aggregate modeling framework in Section III to a French national case study. During cold periods, simultaneous heating leads to an increase in national electricity consumption and hence creates system stress. As a consequence, system operators, including the French transmission system operator – Réseau de Transport d'Électricité (RTE), show growing interest in demand-side flexibility as a strategy to reduce winter peak demand [15]. Applying the proposed model in a national power system context exemplifies how this approach captures large-scale electrified heating behavior.

A. Parameter estimation

We combine national electricity consumption data with population-weighted outdoor temperature observations to estimate the aggregate building thermal resistance. The consumption data at hourly resolution for France in 2023 are obtained from RTE [16]. Hourly outdoor air temperature data for eight weather stations are obtained from the AERIS, Atmosphere Data and Services Centre [17]. These stations correspond to three French standardized climate zones (H1, H2, and H3) defined under the European Commission's Revised thermal regulation (RE2020) [18] to capture regional heterogeneity. Due to inconsistent observations in the Marignane station dataset, we replace it with the *Oikolab*'s hourly temperature data [19]. 2023 regional population data are obtained from the National Institute for Demographic Studies (INED) to compute population-weighted temperatures by mapping administrative regions to stations [20]. In this way, the preprocessed data reflect both spatially and demographically representative conditions across France.

Following the methodology detailed in Section III-B, to isolate heating-dominated periods, we define an indoor-outdoor temperature difference as $\Delta T_t = T^{in} - T^{out}_t$, where T^{in} is fixed at 21°C. We then restrict the regression analysis to observations satisfying $\Delta T_t \geq \Delta T_{\min}$, where $\Delta T_{\min} = \{0, 7, 10, 12\}$°C; for example, a threshold of 7°C implies that heating is activated only when the outdoor temperature is at least 7°C below the indoor setpoint. For each threshold, a linear regression of electricity demand on ΔT_t is performed. We notice that as $\Delta T_{\min}$ increases starting from 7°C, the estimated slope becomes less sensitive to the threshold choice, indicating convergence toward mainly heating behavior, visualized in Fig. 1. $\Delta T_{\min} = 7$°C is therefore selected for the subsequent analysis. We assume an average COP of 1 with 4.3 million electrically heated buildings based on the reported heat pumps statistics from the European Commission in 2022 [21]. Combining (18) and (19), it gives estimates of thermal resistances, $R^{bldg,agg} \approx 5.85 \cdot 10^{-7}$°C/kW, and $R^{bldg} \approx 2.52$°C/kW.

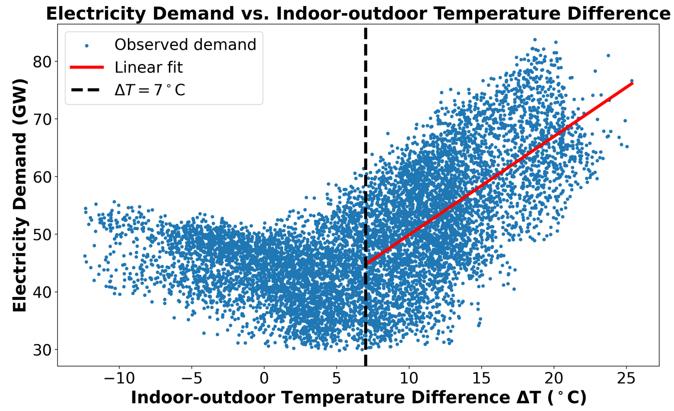

Fig. 1. French national electricity consumption plotted against the indoor-outdoor temperature difference in 2023. Blue points represent observed hourly load, and the red line shows the linear fit obtained using only observations with $\Delta T \geq 7$°C (vertical dashed line).

The remaining parameters are based on standard French residential units and product manufacturer data. Fixed building thermal capacitance, 1.62 kWh/°C, is estimated according to the national average dwelling size of 100 m^2 with ceiling heights of 3 m [22]. Air-to-air and air-to-water heat pumps are modeled with relative shares of 7:3 [23]. Electrical and thermal power limits for air-to-air and air-to-water heat pumps are chosen as 3 kW and 7 kW. Air-to-water heat pumps are parameterized with a 200 L buffer tank with thermal resistance 703.05°C/kW and thermal capacitance 0.23 kWh/°C. Tank temperatures are bounded between 30–55°C, with the ambient temperature of 20°C. In addition, heat pumps' COPs are modeled using piecewise linear functions according to manufacturer specifications. We also include 3 kW resistive heaters which are available in each building with unit efficiency.

B. Simulation setup

To compare the aggregate model performance against the MC benchmark, we consider two heating days (24 hours at 15 minute resolution) – a mild day with a mean outdoor temperature of 11°C (range 8–14°C) when heating starts to be activated based on the R estimation threshold $\Delta T_{\min} = 7$

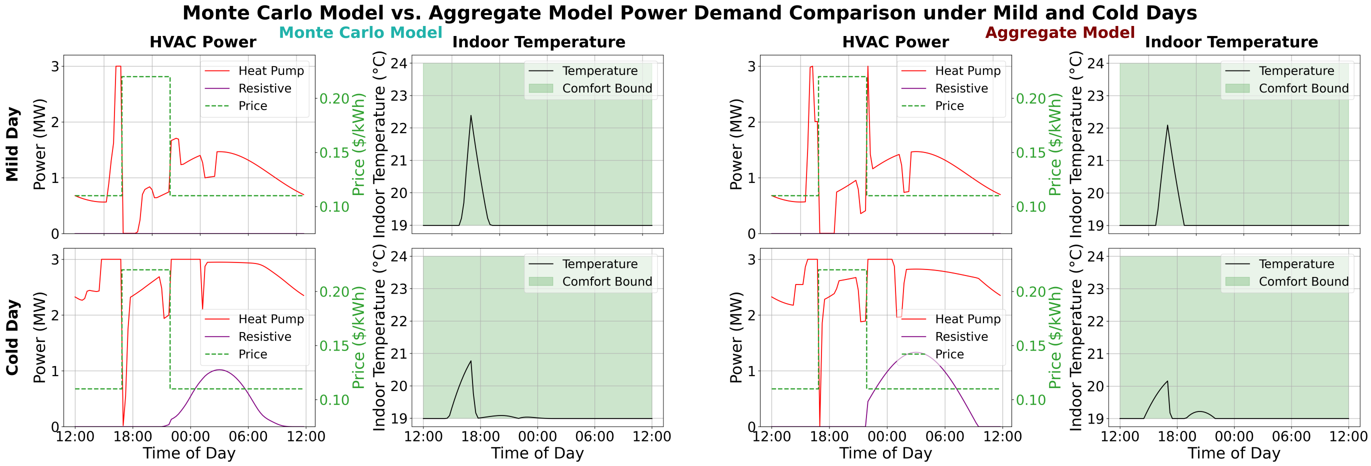

Fig. 2. Comparison of HVAC power demand and indoor temperature between the MC and aggregate models under mild (11°C) and cold (1°C) day scenarios.

and a cold day of high demand with a mean temperature of 1°C (range -2–4°C). For both cases, the outdoor temperature profile follows a synthetic sinusoidal function with 3°C diurnal amplitude, resulting in average heat pump COPs of 3.25 for the mild day and 2.62 for the cold day. Electricity prices include one high price period of $0.22/kWh from 17:00 to 22:00 corresponds to the typical residential peak consumption and $0.11/kWh for all other hours. To ensure computational practicability of the MC benchmark, the total number of buildings N_{hp} is set to be 1,000. Indoor preferred lower and upper bounds are sampled with the means of 19°C and 24°C. All simulations are solved using the Gurobi Optimizer (version 12.0.3) through its Python interface and run on a MacBook Pro with an Apple M-series processor.

V. Results

The proposed aggregate model is applied to the French case study described above. Its performance is evaluated against the MC model with respect to thermal dynamics, modeling accuracy, and computational time. The results also examine the thermal storage tank behavior within the aggregate framework. Fig. 2 compares the aggregate HVAC power consumption (broken down into heat-pump and resistive heating) and indoor temperature over a 24-hour period under mild and cold day scenarios for both the MC and aggregate models in response to electricity price signals.

In both cases, the aggregate model reproduces the main operational patterns observed in the MC model. Prior to high-price periods, both models exhibit preheating behavior which temporarily raises indoor temperatures toward the upper comfort bound to create a thermal buffer. During high-price periods, heating power decreases and indoor temperature gradually approaches the lower comfort bound. Once prices decline, heating resumes at the minimum level required to maintain comfort. These dynamics are more noticeable under cold-day conditions due to higher heating demand. In this case, heating frequently operates near its upper limits to maintain temperature within the comfort range, and resistive heaters are activated when necessary to prevent violation of the minimum indoor temperature constraint.

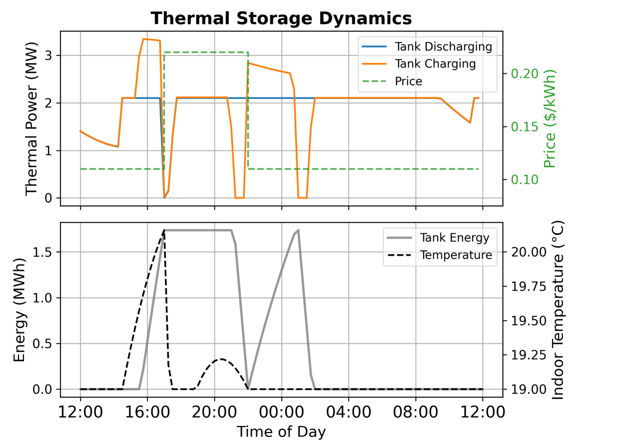

Fig. 3. Thermal storage dynamics of water tanks in the aggregate model under the cold (1°C) day scenario. The upper panel shows tank charging and discharging power with the electricity price signals. The lower panel shows the stored thermal energy and indoor temperature.

To further understand the mechanisms driving this demand response, Fig. 3 illustrates the thermal storage dynamics of the water tanks in the aggregate model under the cold day scenario. Before the price spike, the tank charges as the heating output increases. As a result, stored thermal energy increases and approaches its capacity just before the price spike, following the rise in indoor temperature with a lag due to thermal interaction between space heating and the storage medium. During the high-price period, the system discharges stored energy to support space heating and reduce electricity consumption. Near the end of the peak period, tank energy approaches its minimum level and remains relatively low afterward. Under highly stressed conditions, air-to-water systems exhibit similar behavior to direct space heating, as maintaining indoor temperature becomes the main priority. However, during less constrained periods, the water tanks act as a thermal buffer that shifts the electricity consumption away from peak-price periods.

Differences between these two models are mainly observed in short-term power fluctuations. The aggregate model exhibits larger power spikes, as the aggregate optimization allows

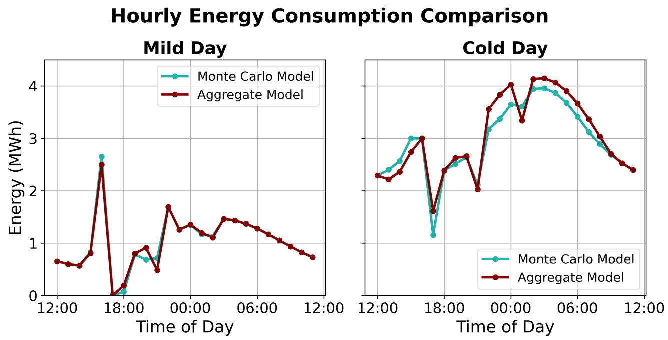

Fig. 4. Hourly aggregate energy consumption comparison between the MC and aggregate models under mild (11°C) and cold (1°C) day scenarios.

heating demand to respond collectively. The MC model, on the other hand, captures heterogeneous individual behavior, which smooths the power demand over time. Despite these differences, the aggregate model preserves major operational trends, which is clearer when examining the hourly energy consumption visualized in Fig. 4. Specifically, the Root Mean Square Error (RMSE) of hourly energy consumption is 0.23 MWh for the cold day and 0.08 MWh for the mild day, corresponding to relative RMSE values of 7.81% and 7.64% when normalized by the average MC energy consumption. The Mean Absolute Errors (MAE) are 0.18 MWh and 0.04 MWh. Moreover, the MC model requires 5.21 s and 5.72 s for the cold day and mild day, whereas the aggregate model solves in only 0.04 s and 0.02 s. As the hourly time resolution is suitable for planning applications and system-level studies, these results indicate the aggregate model provides an accurate and computationally efficient representation of large-scale heating demand.

VI. Conclusion

This paper presents an aggregate thermal modeling framework to quantify system-level flexibility of residential heating systems and remain both physically grounded and computationally efficient for large-scale power system applications. Using a French case study, the aggregate model reproduces the main operational patterns observed in the MC model. The hourly relative RMSE is 7.81% for a cold day and 7.64% for a mild day, and the computational time is reduced from about 5.5 s for the MC model to 0.03 s for the aggregate model. These results demonstrate the aggregate formulation provides an efficient and accurate tool for analyzing residential heating flexibility under price-responsive operation and thermal dynamics. It should be noted that this proposed method could also be used to model aggregate cooling demand in a summer peaking system.

Acknowledgements

We appreciate the support of Power Systems Engineering Research Center (PSERC) Award S-113 and our collaborators from RTE, particularly Olivier Lebois and David Ripayre.

References

[1] Priyadarshan, C. Crozier, K. Baker, and K. J. Kircher, "Distribution grids may be a barrier to residential electrification," Cell Reports Sustainability, vol. 2, no. 11, p. 100518, November 2025.

[2] D. S. Callaway and I. A. Hiskens, "Achieving controllability of electric loads," Proceedings of the IEEE, vol. 99, no. 1, pp. 184–199, January 2011.

[3] D. B. Crawley et al., "EnergyPlus: creating a new-generation building energy simulation program," Energy and Buildings, vol. 33, no. 4, pp. 319–331, April 2001.

[4] M. M. Hossain, T. Zhang, and O. Ardakanian, "Identifying grey-box thermal models with Bayesian neural networks," Energy and Buildings, vol. 238, p. 110836, May 2021.

[5] C. Vallianos, J. Candanedo, and A. Athienitis, "Application of a large smart thermostat dataset for model calibration and model predictive control implementation in the residential sector," Energy, vol. 278, p. 127839, September 2023.

[6] J. A. de Chalendar, C. McMahon, L. Fuentes Valenzuela, P. W. Glynn, and S. M. Benson, "Unlocking demand response in commercial buildings: empirical response of commercial buildings to daily cooling set point adjustments," Energy and Buildings, vol. 278, p. 112599, January 2023.

[7] B. Goetzler, M. Guernsey, and T. Kassuga, "Grid-interactive efficient buildings technical report series: heating, ventilation, and air conditioning (HVAC); water heating; appliances; and refrigeration," December 2019.

[8] C. Crozier, A. Pigott and K. Baker, "Price perturbations for privacy preserving demand response with distribution network awareness," IEEE Transactions on Smart Grid, vol. 15, no. 2, pp. 1584–1593, March 2024.

[9] J. L. Mathieu, M. G. Vayá and G. Andersson, "Uncertainty in the flexibility of aggregations of demand response resources," IECON 2013 - 39th Annual Conference of the IEEE Industrial Electronics Society, November 2013, pp. 8052–8057.

[10] Z. Dong, X. Zhang, L. Zhang, S. Giannelos, and G. Strbac, "Flexibility enhancement of urban energy systems through coordinated space heating aggregation of numerous buildings," Applied Energy, vol. 374, p. 123971, November 2024.

[11] I. M. Granitsas et al., "Controlling air conditioners for frequency regulation: a real-world example," IEEE Transactions on Smart Grid, vol. 16, no. 2, pp. 1221–1232, March 2025.

[12] D. Kim, A. K. Karngala and L. Xie, "Estimation of peak demand reduction using smart thermostats: a Texas case study," 2025 IEEE PES Grid Edge Technologies Conference & Exposition (Grid Edge), January 2025, pp. 1–5.

[13] H. Li, Z. Wang, T. Hong, and M. A. Piette, "Energy flexibility of residential buildings: a systematic review of characterization and quantification methods and applications," Advances in Applied Energy, vol. 3, p. 100054, August 2021.

[14] K. J. Kircher, "Distributed energy resources lecture notes," kevinjkircher.com/distributed-energy-resources/.

[15] Réseau de Transport d'électricité, "Barometer of French demand-side flexibility," RTE, October 2024.

[16] Réseau de Transport d'électricité, "éCO2mix – all of France's electricity data in real time," rte-france.com.

[17] AERIS Atmosphere Data and Services Centre, "Observation data from the Météo-France ground-based observation network," www.aeris-data.fr.

[18] European Commission, "Revised thermal regulation (RE2020)," reforms-investments.ec.europa.eu.

[19] Oikolab, "Weather and climate data API for analysts," oikolab.com.

[20] French National Institute for Demographic Studies (INED), "Population by region," ined.fr.

[21] J. Volt, J. C. Roca Reina, J. Carlsson, and A. Toleikyte, "Heat pump market: country fiches," European Commission, May 2024.

[22] Eurostat, "Average size of dwelling by household composition and degree of urbanisation," ec.europa.eu.

[23] F. Durier, "National report France 2023," IEA Technology Collaboration Programme on Heat Pumping Technologies (HPT TCP), December 2023.